

Published in final edited form as:

*Int J Pharm.* 2010 October 15; 398(1-2): 83–92. doi:10.1016/j.ijpharm.2010.07.029.

## EFFECT OF DIFFERENT ENHANCERS ON THE TRANSDERMAL PERMEATION OF INSLUIN ANALOG

K. M. Yerramsetty, V. K. Rachakonda, B. J. Neely, S. V. Madihally, and K. A. M. Gasem\*  
School of Chemical Engineering, Oklahoma State University, Stillwater, OK 74078

### Abstract

Using chemical penetration enhancers (CPEs), transdermal drug delivery (TDD) offers an alternative route for insulin administration, wherein the CPEs reversibly reduce the barrier resistance of the skin. However, there is a lack of sufficient information concerning the effect of CPE chemical structure on insulin permeation. To address this limitation, we examined the effect of CPE functional groups on the permeation of insulin. A virtual design algorithm that incorporates quantitative structure-property relationship (QSPR) models for predicting the CPE properties was used to identify 43 potential CPEs. This set of CPEs was prescreened using a resistance technique, and the 22 best CPEs were selected. Next, standard permeation experiments in Franz cells were performed to quantify insulin permeation.

Our results indicate that specific functional groups are not directly responsible for enhanced insulin permeation. Rather, permeation enhancement is produced by molecules that exhibit positive log  $K_{ow}$  values and possess at least one hydrogen donor or acceptor. Toluene was the only exception among the 22 potential CPEs considered. In addition, toxicity analyses of the 22 CPEs were performed. A total of eight CPEs were both highly enhancing (permeability coefficient at least four times the control value) and non-toxic, five of which are new discoveries.

### Keywords

transdermal; drug delivery; permeation enhancer; insulin

## 1. INTRODUCTION

Non-traditional methods for insulin delivery like insulin pumps, inhalers and pens are gaining importance due to their obvious advantages over traditional delivery methods [1]. Another promising non-traditional alternative is the delivery of insulin through skin using transdermal patches. Transdermal drug delivery (TDD) can minimize problems commonly associated with traditional delivery methods such as, painful administration, patient compliance, liver metabolism, and sustained and controlled delivery [2]. As such, TDD has gained wide acceptance in many therapeutic applications for a wide variety of drugs like nicotine [3] and estradiol [4].

© 2010 Elsevier B.V. All rights reserved.

\*Author to whom all correspondence should be sent: Phone (405)744-5280, Fax: (405) 744-6338, gasem@okstate.edu.

**Publisher's Disclaimer:** This is a PDF file of an unedited manuscript that has been accepted for publication. As a service to our customers we are providing this early version of the manuscript. The manuscript will undergo copyediting, typesetting, and review of the resulting proof before it is published in its final citable form. Please note that during the production process errors may be discovered which could affect the content, and all legal disclaimers that apply to the journal pertain.

However, delivery of protein molecules like insulin has proven to be difficult due to the large molecular size (>3000 Da.) and hydrophilic nature of these molecules to which the human skin provides a very efficient transport barrier [5,6]. Several physical and chemical methods have been developed to improve the permeation of insulin through human skin [7–10]. By far, the most efficient method in enhancing insulin permeation through skin is iontophoresis [7]; however, the economic viability and ease of applicability of chemical approaches, such as the use of chemical penetration enhancers (CPEs), makes them an attractive alternative.

Very few studies involving the use of CPEs for transdermal insulin delivery exist in the literature [8,11]. Further, in these limited studies, traditional CPEs involving either fatty acids or fatty alcohols are employed in tandem with iontophoresis. As such, CPEs in these applications are not mixed in a solution along with insulin. Instead, the skin is pre-treated with the CPE solution for about two hours, and then washed off before placing the insulin solution on the skin. This is inconvenient from the standpoint of the applicability of an insulin patch designed for sustained TDD. More importantly, these CPEs are limited in their ability to increase the permeation of insulin through the skin significantly and/or exhibit toxic effects to the skin. To address these shortcomings, a large number of CPEs (43 CPEs) containing different functional groups were selected to examine the effect of CPE structural variation on insulin permeation. The CPEs were not used for pre-treating the skin; rather, they were mixed with the insulin solution and allowed to remain in contact with the skin.

The 43 CPEs were identified with our virtual design algorithm which combines genetic algorithms (GAs) and quantitative structure-property relationship (QSPR) models for important CPE properties (skin permeation, octanol-water partition coefficient, melting point, aqueous solubility, and skin sensitization).

Specifically, the development of the virtual design algorithm included (a) integration of non-linear, theory-based structure-property relationship (SPR) property models and genetic algorithms (GAs) to develop a reliable virtual screening algorithm for generation of potential CPEs, and (b) validation of the virtual screening predictions (using melatonin as an example drug and pig skin as the model for human skin) by performing carefully designed experiments for CPE toxicity and drug permeation in the presence of potential CPEs identified as non toxic.

Details concerning the algorithms and models can be found elsewhere [12]. Based on functional group attachments, this set of CPEs was classified as: fatty acids, fatty ketones, fatty alcohols, fatty aldehydes, fatty amines, pyridines/pyrrolidones/pyrrolidinones, alkanes/alkenes/alkynes, halogenoalkanes/alkenes and other miscellaneous CPEs not belonging to any of the previous groups. Only molecules that had positive logarithmic octanol-water partition coefficient ( $\log K_{ow}$ ) values were selected because these molecules are more likely to exhibit desired skin transport properties. As such, only molecules that increase the permeation of drugs through the “pull” mechanism proposed by Liron *et al.* [13] and Kadir *et al.* [14] have been investigated. The permeation effect of this mechanism results from the interaction of a suitable CPE with skin which alters the dermal properties allowing increased permeation of a drug of interest. Significant properties of the CPEs calculated using ChemAxon software [15] are tabulated in Table 1.

The traditional permeation experimental apparatus using Franz diffusion cells provides a reliable *in vitro* technique for estimating the permeation of insulin through the skin; however, it is time and labor intensive. Therefore, a two-step approach for identifying potential CPEs is employed. First, only those CPEs that decrease the skin resistance beyond a threshold value were selected using a resistance technique, which is justified based on our

previous experience and similar studies reported in literature [16–18]. Second, traditional permeation experiments were performed to calculate accurately the permeability of insulin.

Another important issue associated with the use of CPEs is their toxicity. In fact, toxicity is often the major limiting factor in identifying potential CPEs [16]. To assess the suitability of the CPEs investigated in the present study, 3-(4,5-dimethylthiazol-2-yl)-2,5-diphenyltetrazolium bromide (MTT)-formazan assay was employed to evaluate cell viability in the presence of a CPE of interest, and this constituted a preliminary screening mechanism to eliminate CPEs that were toxic at the cellular level. Additionally, histology studies on the intact porcine skin were performed to examine the effects of CPEs on skin.

## 2. MATERIALS AND METHODS

### 2.1. Materials

All of the enhancers studied were obtained from Sigma Aldrich Chemical Company (St Louise, MO, USA), except for 1-methyl-2-pyrrolidone, which was obtained from ConocoPhillips (Bartlesville, OK, USA). Lispro, a short acting analog of human insulin, was purchased from Eli Lilly Company (Indianapolis, IN, USA). Lispro was selected because of its higher dermal absorption rate than normal insulin, which makes it more suitable for transdermal delivery. Henceforth, in the present work, insulin refers to the Lispro analog. Ethanol USP was obtained from Aaper Alcohol and Chemical Co. (Shelbyville, KY, USA). High performance liquid chromatography (HPLC) grade acetonitrile was purchased from Fischer Scientific (Atlanta, GA, USA).

### 2.2. Skin Preparation

Fresh porcine abdominal skin was obtained from Ralphs Packing Co. (Perkins, OK, USA) and Bob McKinney & Sons (Cushing, OK, USA). The skin was cleaned with cold running water to remove dried blood and dirt, and hair was clipped using an electric clipper. The adipose tissue and subcutaneous muscle layers were surgically excised. The skin was then wrapped in aluminum foil and stored at  $-20^{\circ}\text{C}$  until needed. The skin was stored for a maximum of 4 weeks before being used for experimentation. Representative samples were assessed histologically to assess the quality of the skin preparation, as described in Section 2.6.

### 2.3. Prescreening of Enhancers Based on Changes in Skin Resistance

**Preparation of Solution**—Phosphate buffered saline (PBS, pH = 7.4, phosphate and sodium chloride concentrations of 0.001M and 0.137M, respectively) was used to prepare CPE solutions on the day of the experiment. First, 0.5 mL of ethanol was mixed with 0.5 mL of PBS and the test CPEs were added to each of these solutions to give a final CPE concentration of 5% w/v.

**Experimentation**—The enhancers were prescreened based on their skin resistance reduction, which was measured using a resistance chamber that was built in-house. A schematic of the chamber and specific details of this technique, including the current type, the current intensity and the instrumentation are described elsewhere [18]. Briefly, the resistance chamber consists of two half-inch thick Teflon plates fixed to a Teflon Petri dish. Five holes with a diameter of 0.79 cm were drilled into each Teflon plate. The holes in the top plate serve as donor chambers, and the holes in the bottom plate serve as receiver chambers, as in Franz diffusion cells. Porcine skin was placed between the receiver and donor plates with the stratum corneum facing the donor wells, and the two plates were clamped together tightly. The Petri dish was filled with PBS such that the receiver chambers were completely filled with PBS, which was assured by checking the skin resistance;

presence of air pockets between the skin and the receiver chambers showed very high resistance values since air has low conductivity. Resistance readings were taken using a common electrode placed beneath the receiver plate and the other placed sequentially into each donor well, which were filled with just the CPE and no insulin.

All potential enhancers were tested at a concentration of 5% (wt/v) in 1:1 PBS and ethanol solution with the receiver chambers maintained at  $37 \pm 1^\circ\text{C}$ . Resistance measurements were taken every hour for up to 6 hours and the CPE solution was in contact with the skin for this entire period. Rachakonda *et al.* [18] have shown that the efficacy of a CPE can be established by measuring the drop in the skin resistance during a 6 hour contact period between the CPE and the skin. Measurements beyond this time period contribute no additional information regarding CPE efficacy. The resistance reduction factor (RF), which is defined as the ratio of the initial resistance value (R) at time 0 to the resistance value of the sample obtained at time t (6 hrs), was calculated as given by:

$$RF = \frac{R_0}{R_t} \quad (1)$$

#### 2.4. Permeation Experiments on the Prescreened Enhancers

**Preparation of Solution**—Phosphate buffer (PB, pH – 7.4, monosodium phosphate monohydrate and disodium phosphate heptahydrate concentrations of 13.55 mM and 46.41 mM, respectively) was used as the receiver solution in the Franz permeation cells. Solutions of CPEs were prepared on the day of the experiment by dissolving 0.6 mL volume of ethanol with 0.4 mL of insulin solution. The final concentration of insulin was approximately 40 IU/mL or 1.8 mg/mL. The test CPEs were added to each of these solutions to give a final concentration of 5% w/v. In general, the enhancement effect is dependent on the concentration of the CPE in the donor solution, and if a CPE was to be developed commercially, a range of concentration for each CPE would require investigation. However, due to the number of CPEs involved in this work, we have limited testing to CPEs only at a 5% w/v concentration. The enhancement at this concentration has been used widely in skin permeation literature as a reasonable indicator of the CPE's efficacy [19–21].

**Experimentation**—All the permeation experiments were conducted using Franz diffusion cells (PermeGear Inc., Riegelsville, PA, USA). The capacities of the donor and the receiver chambers were 1 mL and 5 mL, respectively. The surface area available for diffusion was  $0.64 \text{ cm}^2$ . The receiver chamber temperature was maintained at  $37 \pm 1^\circ\text{C}$  using a flow loop consisting of a water bath reservoir (Isotemp 105, Fischer, Atlanta, GA, USA) and a Masterflex L/S peristaltic pump (Fischer, Atlanta, GA, USA).

The receiver chambers of the Franz diffusion cells were filled with PB and stirred continuously using a magnetic stir bar. Abdominal skin was thawed at room temperature for a minimum of two hours and was placed between the donor and receiver chambers with the stratum corneum facing the donor chamber. Then, 1.0 mL solutions containing insulin and CPE were placed inside the donor chambers of Franz diffusion cells. The control samples contained 0.4 mL insulin and 0.6 mL ethanol solution. At different time intervals (3, 9, 12, 18, 24, 36 & 48 h), 0.1 mL samples were withdrawn from the receiver chamber using a syringe. Fresh PB in 0.1 mL amounts was replaced in the receiver chambers. The collected samples were stored at  $4^\circ\text{C}$  until further analysis.

**HPLC Analysis**—The concentrations of insulin in the receiver chambers at different time intervals were measured using a HPLC system (Dionex Co., Sunnyvale, CA, USA) containing a Waters Symmetry 300 column (4.6 \* 150 mm dimensions,  $5 \mu\text{m}$  and  $90 \text{ \AA}$

packing). A 40:60 (v/v) mixture of acetonitrile and water was the mobile phase. Flow rate was 1.0 mL/min and the eluent was monitored at 276 nm. Linearity for HPLC analysis was observed in the concentration range of 0.01–12.5 IU/mL ( $R^2 > 0.99$ ).

**Permeability Coefficient ( $K_p$ ) and Enhancement Factor (EF) Calculations**—The following steady-state equation was used to calculate permeability of the skin:

$$\text{Amount of drug permeated} = A_m \cdot C_0 \cdot K_p \cdot t \quad (2)$$

where,  $A_m$  is the exposure area of the skin sample ( $0.64 \text{ cm}^2$ ),  $C_0$  is the initial concentration in the donor chamber in mM,  $K_p$  is the permeability of the membrane and  $t$  is time in hrs. The permeability is given in terms of the diffusion coefficient ( $D_m$ ), the partition coefficient ( $K_m$ ), and the thickness of the skin sample ( $L$ ):

$$K_p = \frac{D_m K_m}{L} \quad (3)$$

In this study, the amount of drug permeated was calculated as the total amount of drug permeated through skin during a time period of 48 hr. The lag times ( $L_t$ ) were calculated as the x-intercept of the steady-state portion of the permeation profiles (cumulative insulin permeated, IU/cm<sup>2</sup>) plotted against the time (hr) profiles, as shown in Figure 1.

## 2.5. In Vitro Cytotoxicity Analysis

Human foreskin fibroblasts (HFF-1, cell line) were purchased from American Type Culture Collection (Walkersville, MD, USA) and maintained in Dulbecco's Modified Eagle Medium supplemented with 4 mM L-glutamine, 4.5 g/L sodium bicarbonate, 0.1 mM  $\beta$ -mercaptoethanol, 100 U/mL penicillin-streptomycin, 2.5 g/mL amphotericin, and 10% Fetal bovine serum (Invitrogen Corp., Carlsbad, CA, USA). The cell cultures were maintained in 5% CO<sub>2</sub> at 37°C with medium changes every 48 h.

Cells in the exponential growth phase were detached using 0.05% trypsin - 10  $\mu$ M ethylenediaminetetraacetic acid (EDTA) (Invitrogen Corp., Carlsbad, CA, USA), centrifuged, and re-suspended in fresh growth medium. Viable cells were counted in a hemocytometer using trypan blue dye exclusion principle, and approximately 25,000 viable cells were seeded into each well of a 24-well plate in 0.5 mL growth medium and incubated for 24 h. CPEs were dissolved in PBS with 1% dimethyl sulfoxide (DMSO). The CPEs were tested at three different concentrations of 10 mg/mL, 1 mg/mL and 0.1 mg/mL.

After 24 h of exposure to the CPEs, morphological changes were monitored using an inverted microscope (Nikon, TE2000U, Melville, NY), and digital micrographs were captured from different locations on the well plate. Additionally, MTT assays were performed for viability testing using a previously reported procedure [22]. In brief, growth medium was replaced with 0.5 mL of 2 mg/mL MTT (Sigma-Aldrich Chemical Company, St. Louis, MO, USA) solution in PBS and incubated for four to five hours at 37°C. The MTT solution was discarded, the cells were washed with PBS solution, and 0.2 mL DMSO was added to dissolve the formazan salt crystals. The absorbance of the solution containing the solubilized formazan was measured at 540 nm with readings at 620 nm serving as references. Fraction viabilities for each well were calculated with respect to the control wells using the following equation.

$$\text{Fraction viability} = \frac{\text{Abs}(540) - \text{Abs}(620)}{\frac{\sum_{i=1}^n \{\text{Abs}(540) - \text{Abs}(620)\}_{\text{control}}}{n}} \quad (4)$$

where, Abs(540) and Abs(620) indicate the absorbance values for the well at 540 nm and 620 nm, respectively, n indicates the number of wells used as controls (replicates) and the subscript control indicates the readings of the control wells.

## 2.6. Histology

Skin samples that were used for the permeation studies were immediately removed from the Franz cells and fixed in 1.5% buffered formalin. The samples were embedded in paraffin and 6- $\mu\text{m}$  sections were cut using a microtome. Hemotoxylin and eosin staining was performed and digital photomicrographs were taken at representative regions using an inverted microscope (Nikon, TE2000U, Melville, NY, USA).

Morphological changes in the skin (especially in epidermal layers) after the permeation experiments were observed visually and classified on a scale of A–D; Class A – non toxic (morphology of the sample looks exactly similar to the control sample); Class B – slightly toxic (morphology looks almost similar to the control sample); Class C – toxic (morphology includes partial epidermal degradation with nuclei bleeding into the dermal layers); Class D – severely toxic (morphology includes severe epidermal degradation with cell death).

## 2.7. Statistical Analysis

All experiments were performed at least three times, and single factor one-way analysis of the variance (ANOVA) was performed with a 95% confidence interval on the cell fraction viability and drug permeability data. This was done to determine if the differences among these data at different experimental conditions are greater than the errors due to random effects. A *p*-value less than 0.05 indicates a significant difference exists between the two groups of data.

## 3. RESULTS

### 3.1. Prescreening of the Enhancers

A total of 43 enhancers were tested for reduction in porcine skin resistance using the resistance technique. The calculated reduction factors of the candidate CPEs are tabulated in Table 2. Only those enhancers that caused a reduction factor of 10 or greater were marked as effective and selected for further analysis. These CPEs (a total of 22) are marked with an asterisk, as shown in Table 2. Different CPEs belonging to all the functional group classes except for the “alkanes/alkenes/alkynes” group were represented in these 22 prescreened enhancers. No particular functional group contributed dominantly to this list of pre-screened enhancers, and molecular structures not satisfying the pre-screening criterion were represented by all group classes.

### 3.2. Permeability of Insulin in the Presence of the Prescreened Enhancers

To evaluate the permeation of insulin in the presence of the prescreened enhancers, permeation experiments were performed using the standard Franz diffusion cells. The cumulative amounts of insulin permeated per  $\text{cm}^2$  and the permeability values ( $K_p$ ) are tabulated in Table 3. From the table, it is evident that all the enhancers with a RF of at least 10 also increased cumulative amount of insulin permeated by at least two times ( $\text{EF} > 2$ ).

This provides validation of our prescreening procedure using the resistance technique. No functional group exhibited significantly high permeabilities when compared to other groups. Table 3 also lists the lag times,  $L_t$  for permeation in the presence of CPEs. All CPEs except for lauric acid and toluene increased the lag time when compared to the lag times obtained using the control (ethanol + insulin) solution. The lag times in the presence of lauric acid are comparable to the control value, while the lag times in the presence of toluene were significantly lower than the control value.

The relationship between  $K_p$  and RF values was explored; however, initial results showed large deviations for two CPEs, 2,3-dichloro-1-propene and toluene, which were excluded from further analysis. Subsequently, a correlation plot of averaged  $\log K_p$  and  $\log RF$  values, where values were averaged at approximately 0.1  $\log RF$  intervals, was plotted (Figure 2) and the resulting  $R^2$  was found to be 0.79. A horizontal line in the figure indicates the  $K_p$  value for the control. As shown in the figure and Table 3, all the prescreened enhancers had  $K_p$  values greater than that of control, indicating that the prescreening resistance technique is able to predict successfully the CPEs that might enhance permeation of insulin.

### 3.3. Cytotoxicity of Predicted CPEs

At the highest concentration of 10 mg/mL all the CPEs exhibited toxicity (fractional viability less than 0.3; data not shown); even though in the cases of 4-octanone and octaldehyde, the morphology and the density of the cells was similar to that of control. At the lowest concentration of 0.1 mg/mL all the enhancers except for pulegone (fractional viability < 0.3) were found to be non-toxic (fractional viability was statistically similar to control,  $p > 0.05$ ; data not shown). At the moderate concentration of 1 mg/mL, eight enhancers were found to be non-toxic as shown in Figure 3. The figure presents toxicity in terms of fractional viability with respect to control after 24 h of cell exposure to CPEs, as assessed using the MTT assay. Of the 22 CPEs examined, satisfactory viability (fractional viability was statistically similar to control,  $p > 0.05$ ) was indicated for eight CPEs: menthone, decanol, oleic acid, *cis*-4-hexen-1-ol, 2,4,6-collidine, cycloundecanone, 4-octanone, and octaldehyde. All other CPEs showed significant reduction in the viability of cells ( $p < 0.05$ ). To understand the influence of CPEs on cellular activity, morphology of fibroblasts was assessed after 24 h of exposure to CPEs found to be non-toxic after MTT assays. The micrographs of the cells (upper panels) are provided in Figure 4 along with the micrographs of the skin (lower panels) after exposure to each CPE. These results show that the addition of these CPEs did not alter cell morphology, indicating that the CPE had no toxic effects.

### 3.4. Histology of Skin Exposed to CPEs

Micrographs of the porcine skin after exposure to CPEs are given in the lower panels of Figure 4. Table 4 shows the CPEs graded according to their effect on the morphology of the skin, as mentioned in Section 2.6. There was severe epidermal degradation with complete cell death for skin exposed to menthone, indicating a high level of toxicity (classified as D). Decanol was slightly toxic (classified as B) to the skin cells as shrunken nuclei in the epidermal layers were observed. Cycloundecanone was moderately toxic (classified as B) with nuclei from the epidermis bleeding slightly into the dermis. In contrast, oleic acid, 4-octanone, octanal, *cis*-4-hexen-1-ol and 2,4,6-collidine were nontoxic (classified as A) as no significant change in the morphology of the skin samples exposed to the respective chemicals was observed.

## 4. DISCUSSION

Traditional methods of identifying CPEs usually involve laborious and time-intensive permeation measurements that reduce significantly the experimental throughput. An alternative has been proposed in the literature [16,17] that uses the changes in electrical resistance to estimate the enhancement effect of the CPEs. This method is more efficient in terms of cost and time when compared to permeation experiments. Therefore the resistance technique was employed in the present work to prescreen the initial list of 43 molecules. A total of these 22 enhancers were examined further using the traditional permeation experiments involving Franz diffusion cells and HPLC. The lag times in the presence of most CPEs were found to be greater than the lag time in the presence of control (ethanol + insulin) solution. This could be due to the length of time involved in the stratum corneum permeation by higher molecular weight CPEs when compared to the lower molecular weight ethanol. Also, no relationship was found between the resistance reduction profiles (not shown) and the calculated lag times.

The resistance reduction factor and enhancement factor were calculated for these 22 pre-screened enhancers, and the observed correlation ( $R^2 = 0.79$ ) between the enhancer RF and  $K_p$  values is shown in Figure 2. Variation in the correlation can be attributed to the limited number of data, the variable initial resistances of different skin samples, hair density on that particular skin sample and other factors that lead to large uncertainties in the reduction of resistances [23–25]. Although, great care has been taken to limit these uncertainties (including the use of select abdominal skin samples that have a narrow range of initial resistance values), variations due to other factors such as age, weight and previous history of the animal usually associated with biological samples could not be avoided. In addition, limiting the resistance experiments to 6 h to enhance the experimental throughput magnifies these uncertainties. Therefore, the resistance technique should be used as a “coarse” rapid method for identifying CPEs that alter significantly the barrier properties of the skin. The exact level of enhancement should be estimated from the traditional permeation experiments.

The log  $K_{ow}$  values, molecular weights, number of hydrogen donors and acceptors for all of the enhancers are tabulated in Table 1. Of the 43 enhancers tested using resistance technique, all except two enhancers had positive log  $K_{ow}$  values. However, this alone is not a sufficient condition for a chemical to be an enhancer, as is evident from the RF values for the chemicals in the alkanes/alkenes/alkynes group, where a wide range of positive log  $K_{ow}$  values does not translate to significant reduction in skin resistance. Also, these CPEs have not shown any increase in insulin permeation (data not shown). An important aspect of this group of chemicals is their lack of hydrogen acceptors or donors (Table 1), which indicates that these two properties are significant attributes of an effective insulin enhancer. Narishetty and Panchagnula [26,27] have reported that oxygen atoms in the terpenes form hydrogen bonds with skin lipid bi-layers and lead to stratum corneum structure modification. Therefore, it is reasonable to expect that any CPE with hydrogen bonding capability will have the ability to modify the stratum corneum structure. Further studies need to be conducted to investigate the number of hydrogen bonding groups that would result in optimum enhancement. However, we found two exceptions to this hydrogen bonding rule; cetyltrimethyl ammoniumbromide and toluene, both of which enhance the permeation of insulin significantly, but have no hydrogen donors or acceptors. The anomaly exhibited by cetyltrimethyl ammonium bromide can be explained by the fact that it dissociates into an ionic form in aqueous solutions and therefore has some electronegative effects, even though the structure lacks any hydrogen donors or acceptors. This still leaves the behavior of toluene unexplained since electronegative regions in the structure are absent.



Since toxicity is the major limitation of the applicability of the CPEs, all 22 prescreened enhancers were tested for their effects on human fibroblasts at three concentrations of different orders of magnitude (10 mg/mL, 1 mg/mL and 0.1 mg/mL). At the moderate concentration of 1 mg/mL, eight enhancers were found to be non-toxic. In the presence of these non-toxic enhancers, the  $K_p$  value for insulin permeation was at least 4 times that of control. Therefore, our search has resulted in eight CPEs (a) that were non-toxic from the preliminary cytotoxicity studies, and (b) that enhance insulin permeation, as deduced from the *in vitro* permeation studies.

The cellular toxicity (*in vitro*) studies were conducted at 1% w/v whereas the permeation studies and the histology studies were performed at 5% w/v. Using 1 mg/mL (or 1% w/v) CPE for each well of a 24 well plate, the average concentration of the CPE per cell is approximately  $4 \times 10^{-5}$  mg/mL. In the permeation experiments, the average concentration of the CPE per skin cell is approximately  $1.5 \times 10^{-5}$  mg/mL, assuming porcine skin cell density to be equal to that of human skin, which is approximately 6 million cells per square centimeter, and that all of the CPE in the donor solution transports into the viable epidermis. Since the amount of CPE transported into the viable layers of the skin is less than the concentration of CPE in the donor chamber due to the transport barrier presented by the stratum corneum, the value presented above is a conservative estimate for the actual CPE concentration in the epidermis. Therefore, if the CPE was non-toxic at the concentration of  $4 \times 10^{-5}$  mg/mL per cell, then the CPE must be non-toxic in the permeation experiments where the concentration is less than  $1.5 \times 10^{-5}$  mg/mL per cell. The *in vitro* toxicity results presented in the current work can be safely extrapolated to assess the toxicity of the CPE to the skin cells in the permeation experiments.

As discussed previously, the *in vitro* cellular level toxicity data usually overestimates the effect of the CPE on the skin, due to the lack of a proper stratum corneum that acts as the initial barrier to the transport of molecules into the skin [28]. Therefore, the cellular level data provides an approximation of the toxicity of the CPE. While histological analysis is a more reliable toxicity model, this technique is time and labor-intensive and therefore was used only to confirm the cytotoxicity results for the eight non-toxic CPEs. The grading of the CPEs based on their effect on porcine skin is tabulated in Table 4, from which it is evident that seven of the eight potential CPEs are non-toxic to the intact skin; menthone was the exception that shows severe toxicity; nevertheless, when menthone was tested on porcine skin at 1% w/v, it was non-toxic, indicating a concentration-dependent toxicity effect for this CPE in the concentration ranges that we tested for.

Of the eight CPEs discovered in this study, menthone, decanol and oleic acid have already been thoroughly investigated in the literature for their effects on the enhancement of different drugs. Specifically, pre-treatment of the porcine skin with menthone and other terpenes has been used to enhance permeation of insulin in conjunction with iontophoresis [29]. Also, menthone has been used to enhance the permeation of weakly hydrophobic drugs like melatonin [18] and some strongly hydrophobic drugs like tamoxifen [30]. Similarly, decanol and oleic acid have been used as permeation enhancers for a large variety of drugs like melatonin [19,20] and ketotifen [31]. However, to our knowledge, they have not been used to enhance insulin permeation through skin. The remaining five CPEs discovered in this study have not been investigated for their enhancement effects with any drug in the literature previously.

One final note on the validity of the results of this work is in order. In the current work, all data has been generated using *in vitro* methods. However, *in vitro* results are not a true indication of the bioavailability of the drug and the toxicity effects of the CPE. Therefore, *in vivo* studies are required to confirm the safety and applicability of the CPEs identified in this

work. Further, no interactions were assumed between the CPE and insulin in the donor solution, based on the nearly constant elution time observed for insulin during HPLC analysis; however, additional studies need to be performed on potential CPEs to confirm this assumption.

## 5. CONCLUSIONS

The current results lead to the conclusion that no specific CPE functional groups are directly responsible for enhanced insulin permeation. Rather, CPE permeation enhancement is produced by molecules that exhibit positive  $\log K_{ow}$  values and possess at least one hydrogen donor or acceptor, with the exception of toluene among the 22 CPEs considered. As such, future CPE screening could be narrowed down to include only molecules that meet these criteria, thus reducing the computational and experimental burdens involved in identifying new CPEs.

The current work also demonstrates the usefulness of an efficient two-step approach for identifying CPEs, namely, the use of the resistance technique as a rapid method to pre-screen the potential CPEs followed by the traditional permeation measurements to quantify accurately the permeabilities. This approach was used to screen an initial set of 43 potential CPEs to identify 22 likely CPEs, which were then tested for their effect on insulin permeability. Despite its high-throughput, the resistance technique remains a coarse method for identifying potential CPEs and should not be the primary determinant for estimating the increase in drug permeability.

As also shown in the literature, toxicity of discovered CPEs was the major limiting factor in applicability in the current work. Only eight of the 22 potential CPEs that enhanced insulin permeability were found to be non-toxic. Of these eight, three CPEs were investigated previously in the literature, and five CPEs have never been investigated as enhancers.

## Acknowledgments

Financial support for this research was provided by the National Institute of Biomedical Imaging and Bioengineering (1R21EB005749).

## REFERENCES

1. Patni P, Varghese D, Balekar N, Jain DK. Needle-free insulin drug delivery. *Indian Journal of Pharmaceutical Sciences*. 2006; vol. 68:7–12.
2. Chong, S.; Fung, HL. Transdermal drug delivery systems: Pharmacokinetics, clinical efficacy, and tolerance development. In: Hadgraft, J.; Guy, RH., editors. *Transdermal Drug Delivery: Developmental Issues and Research Initiatives*. 1st ed. New York: Marcel Dekker; 1989. p. 135-154.
3. Nair MK, Chetty DJ, Ho H, Chien YW. Biomembrane permeation of nicotine: Mechanistic studies with porcine mucosae and skin. *Journal of Pharmaceutical Sciences*. 1997; vol. 86:257–262.
4. Goodman M, Barry BW. Action of penetration enhancers on human skin as assessed by the permeation of model drugs 5-fluorouracil and estradiol. I. Infinite dose technique. *Journal of Investigative Dermatology*. 1988; vol. 91:323–327. [PubMed: 3171212]
5. Monteiro-Riviere, NA. Comparative anatomy, physiology, and biochemistry of mammalian skin. In: Hobson, DW., editor. *Dermal and Ocular Toxicology: Fundamentals and Methods*. 1st ed. Boca Raton, FL: CRC Press; 1991. p. 3-73.
6. Monteiro-Riviere, NA. Anatomical factors affecting barrier function. In: Marzulli, FN.; Maibach, HI., editors. *Dermatotoxicology*. 1st ed. Washington, D.C.: Taylor & Francis; 1996. p. 43-70.

7. Pillai O, Panchagnula R. Transdermal delivery of insulin from poloxamer gel: *Ex vivo* and *in vivo* skin permeation studies in rat using iontophoresis and chemical enhancers. *Journal of Controlled Release*. 2003; vol. 89:127–140. [PubMed: 12695068]
8. Rastogi SK, Singh J. Passive and iontophoretic transport enhancement of insulin through porcine epidermis by depilatories: Permeability and fourier transform infrared spectroscopy studies. *AAPS PharmSciTech*. 2003; vol. 4:E29. [PubMed: 14621961]
9. Pan Y, Zhao HY, Zheng JM. The enhancing effect of electroporation and iontophoresis on the permeation of insulin through human skin. *Yao Xue Xue Bao*. 2002; vol. 37:649–652. [PubMed: 12567783]
10. Smith NB, Lee S, Shung KK. Ultrasound-mediated transdermal *in vivo* transport of insulin with low-profile cymbal arrays. *Ultrasound in Medicine & Biology*. 2003; vol. 29:1205–1210. [PubMed: 12946523]
11. Pillai O, Nair V, Panchagnula R. Transdermal iontophoresis of insulin: Iv. Influence of chemical enhancers. *International Journal of Pharmaceutics*. 2004; vol. 269:109–120. [PubMed: 14698582]
12. Godavorthy SS, Yerramsetty M, Rachakonda VK, Neely BJ, Madihally SV, Robinson RL Jr, Gasem KA. Design of improved permeation enhancers for transdermal drug delivery. *J Pharm Sci*. 2009; vol. 98:4085–4099. [PubMed: 19697392]
13. Liron Z, Cohen S. Percutaneous absorption of alkanolic acids II: Application of regular solution theory. *Journal of Pharmaceutical Sciences*. 1984; vol. 73:538–542. [PubMed: 6726640]
14. Kadir R, Stempler D, Liron Z, Cohen S. Delivery of theophylline into excised human skin from alkanolic acid solutions: A "Push-pull" Mechanism. *Journal of Pharmaceutical Sciences*. 1987; vol. 76:774–779. [PubMed: 3430340]
15. ChemAxon. Marvin and calculator plugin demo. [last accessed on December, 2007]. <http://www.chemaxon.com/demosite/marvin/index.html>
16. Karande P, Jain A, Mitragotri S. Discovery of transdermal penetration enhancers by high-throughput screening. *Nature Biotechnology*. 2004; vol. 22:192–197.
17. Karande P, Jain A, Mitragotri S. Relationships between skin's electrical impedance and permeability in the presence of chemical enhancers. *Journal of Controlled Release*. 2006; vol. 110:307–313. [PubMed: 16313994]
18. Rachakonda VK, Yerramsetty KM, Madihally SV, Robinson JRL, Gasem KAM. Screening of chemical penetration enhancers for transdermal drug delivery using electrical resistance of skin. *Pharmaceutical Research*. 2008; vol. 25:2697–2074. [PubMed: 18683029]
19. Kandimalla K, Kanikkannan N, Andega S, Singh M. Effect of fatty acids on the permeation of melatonin across rat and pig skin *in-vitro* and on the transepidermal water loss in rats *in-vivo*. *Journal of Pharmacy and Pharmacology*. 1999; vol. 51:783–790. [PubMed: 10467952]
20. Andega S, Kanikkannan N, Singh M. Comparison of the effect of fatty alcohols on the permeation of melatonin between porcine and human skin. *Journal of Controlled Release*. 2001; vol. 77:17–25. [PubMed: 11689256]
21. Kanikkannan N, Singh M. Skin permeation enhancement effect and skin irritation of saturated fatty alcohols. *Int J Pharm*. 2002; vol. 248:219–228. [PubMed: 12429475]
22. Mosmann T. Rapid colorimetric assay for cellular growth and survival: Application to proliferation and cytotoxicity assays. *Journal of Immunological Methods*. 1983; vol. 65:55–63. [PubMed: 6606682]
23. Nicander I, Ollmar S. Electrical impedance measurements at different skin sites related to seasonal variations. *Skin Research and Technology*. 2000; vol. 6:81–86. [PubMed: 11428947]
24. Fujita T, Fujii Y, Okada SF, Miyauchi A, Takagi Y. Fall of skin impedance and bone and joint pain. *Journal of Bone and Mineral Research*. 2001; vol. 19:175–179.
25. Davies DJ, Ward RJ, Heylings JR. Multi-species assessment of electrical resistance as a skin integrity marker for *in vitro* percutaneous absorption studies. *Toxicology In Vitro*. 2004; vol. 18:351–358. [PubMed: 15046783]
26. Narishetty ST, Panchagnula R. Transdermal delivery of zidovudine: Effect of terpenes and their mechanism of action. *Journal of Controlled Release*. 2004; vol. 95:367–379. [PubMed: 15023449]
27. Narishetty ST, Panchagnula R. Transdermal delivery system for zidovudine: *In vitro*, *ex vivo* and *in vivo* evaluation. *Biopharmaceutics & Drug Disposition*. 2004; vol. 25:9–20.

28. Kojima H, Sato A, Hanamura A, Katada T, Konishi H. Evaluation of skin irritation in a reconstituted human dermal model (3-d model) using water insoluble fatty acids, fatty alcohols and hydrocarbons. *Alternatives to Animal Testing and Experimentation*. 1998; vol. 5:201–210.
29. Pillai O, Panchagnula R. Transdermal iontophoresis of insulin. V. Effect of terpenes. *Journal of Controlled Release*. 2003; vol. 88:287–296. [PubMed: 12628335]
30. Zhao K, Singh S, Singh J. Effect of menthone on the in vitro percutaneous absorption of tamoxifen and skin reversibility. *International Journal of Pharmaceutics*. 2001; vol. 219:177–181. [PubMed: 11337177]
31. Kimura C, Nakanishi T, Tojo K. Skin permeation of ketotifen applied from stick-type formulation. *European Journal of Pharmaceutics and Biopharmaceutics*. 2007; vol. 67:420–424. [PubMed: 17433642]

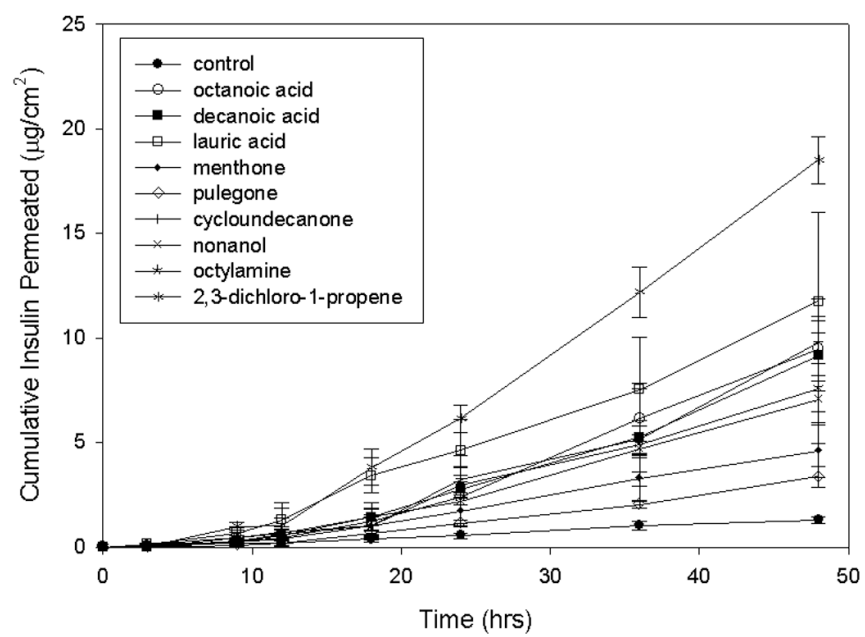


**Figure 1.**  
Permeation profiles of insulin the presence of selected CPEs

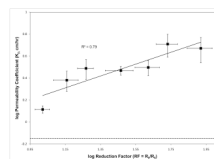


**Figure 2.** Variation of permeability with reduction factor on an averaged basis. The horizontal dashed line indicates the control level. The solid line is the regression line for the correlation between the permeability coefficient and reduction factor.

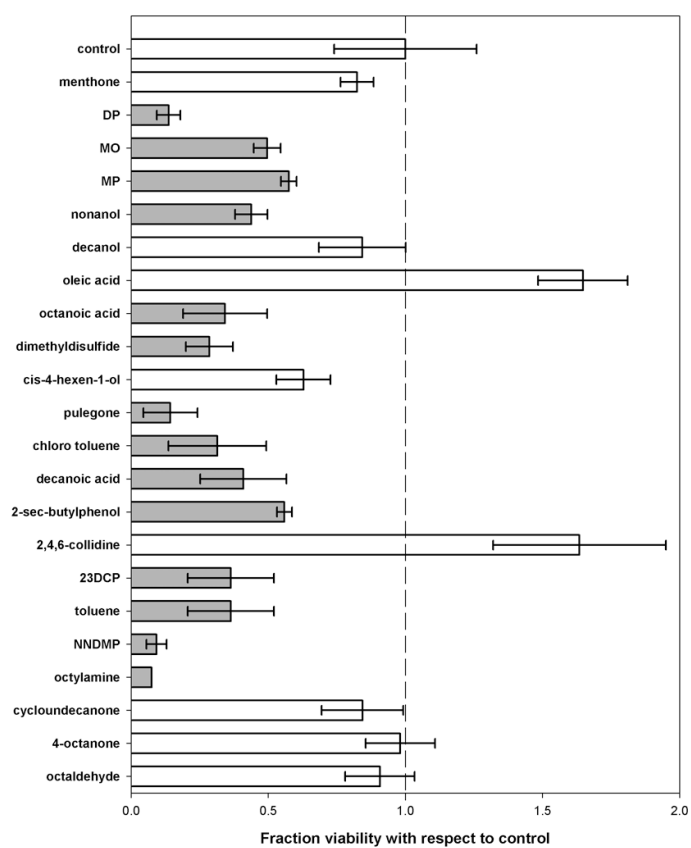


**Figure 3.** Toxicity after 24 hours of exposure to the CPEs. The non-toxic CPEs and toxic CPEs are colored in white and grey, respectively.

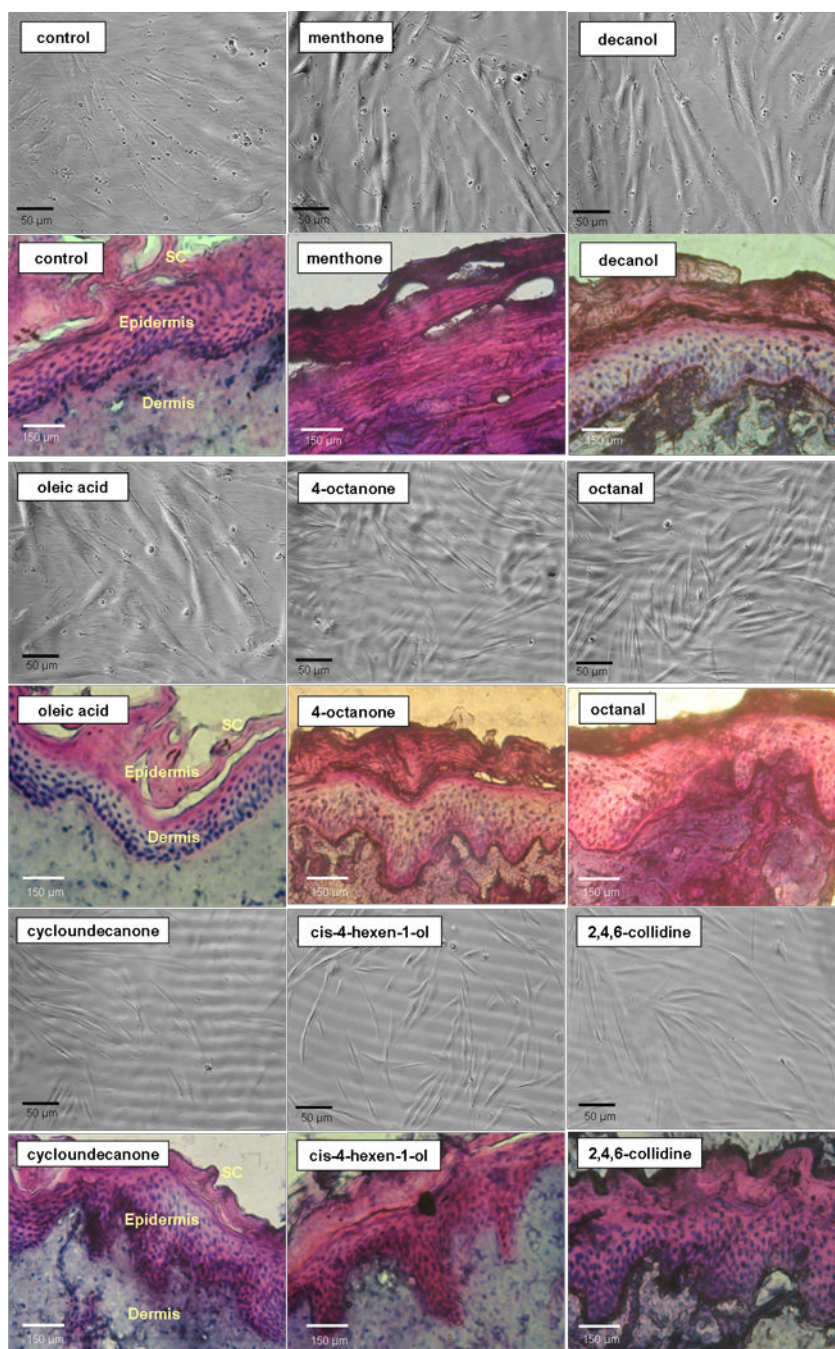


**Figure 4.** Micrographs of the cells (upper panels) and the pig skin samples (lower panels) after exposure to the CPEs at a concentration of 5% w/v.



**Table 1**

Properties of the CPEs tested, where the parenthetical values are indicative of either donor or acceptor sites.

CPE	Octanol-water partition coefficient (log $K_{ow}$ )	MW (Da)	Hydrogen donors (donor sites)	Hydrogen acceptors (acceptor sites)
<b>Acids</b>				
octanoic acid	2.4	144.2	1 (1)	2 (3)
decanoic acid	3.2	172.3	1 (1)	2 (3)
oleic acid	6.1	282.5	1 (1)	2 (3)
lauric acid	4.0	200.3	1 (1)	2 (3)
azelaic acid	1.6	188.2	2 (2)	4 (6)
salicylic acid	1.9	138.1	2 (2)	3 (4)
<i>tert</i> -butyl acetic acid	1.6	116.2	1 (1)	2 (3)
<b>Ketones</b>				
menthone	3.1	154.3	0 (0)	1 (2)
acetophenone	1.4	120.2	0 (0)	1 (2)
4-octanone	2.8	128.2	0 (0)	1 (2)
pulegone	2.8	152.2	0 (0)	1 (2)
cycloundecanone		168.8		
3-methyl-2-hexanone	2.4	114.2	0 (0)	1 (2)
2-methyl cyclohexanone	2.1	112.2	0 (0)	1 (2)
2-heptanone	2.2	114.2	0 (0)	1 (2)
<b>Alcohols</b>				
<i>cis</i> -4-hexen-1-ol	1.2	100.2	1 (1)	1 (1)
nonanol	2.6	144.3	1 (1)	1 (1)
decanol	3.0	158.3	1 (1)	1 (1)
<b>Aldehydes</b>				
hexanal	1.2	100.2	0 (0)	1 (2)
octanal	2.0	128.2	0 (0)	1 (2)
salicylaldehyde	2.1	122.1	1 (1)	2 (3)
<b>Amines</b>				
<i>N,N</i> -dimethylisopropylamine	0.9	87.2	1 (1)	0 (0)
octylamine	2.2	129.2	1 (2)	1 (1)
<b>Pyridines/ Pyrrolidones/Pyrrolidinones</b>				
2,4,6-collidine	1.5	121.2	0 (0)	1 (1)
1-dodecyl-2-pyrrolidinone	4.0	253.4	0 (0)	1 (2)
1-methyl-2-pyrrolidone	-0.4	99.1	0 (0)	1 (2)
2-methyl-3-oxazolidinone	-0.1	101.1	0 (0)	2 (3)
<b>Alkanes/Alkenes/Alkynes</b>				
nonane	5.6	128.2	0 (0)	0 (0)

CPE	Octanol-water partition coefficient (log $K_{ow}$ )	MW (Da)	Hydrogen donors (donor sites)	Hydrogen acceptors (acceptor sites)
cyclopentane	2.0	70.1	0 (0)	0 (0)
1-pentene	2.3	70.1	0 (0)	0 (0)
1-pentyne	1.8	68.1	0 (0)	0 (0)
2-methylbutane	2.4	72.1	0 (0)	0 (0)
<b>Halogenoalkanes/alkenes</b>				
1-bromopropane	1.8	123.0	0 (0)	0 (0)
1,2-dichloropropane	2.0	113.0	0 (0)	2 (2)
2,3-dichloro-1-propene	1.4	111.0	0 (0)	2 (2)
<b>Other</b>				
cetyltrimethyl ammonium bromide	1.5	364.4	0 (0)	0 (0)
2-chlorotoluene	3.0	126.6	0 (0)	1 (1)
toluene	2.5	92.1	0 (0)	0 (0)
dimethyldisulfide	1.3	94.2	0 (0)	2 (2)
2-sec-butylphenol	3.4	150.2	1 (1)	1 (1)
methyl caproate	1.7	130.2	0 (0)	1 (2)
ethyl 2-methylpentanoate	2.2	144.2	0 (0)	1 (2)
ethylbutyrate	1.2	116.2	0 (0)	1 (2)

**Table 2**

Reduction factors (RF) calculated for the enhancers. The data are the means and standard deviations of a minimum of three repetitions. Enhancers marked with an asterisk produced RF values greater than 10

CPE	RF = $R_0/R_6$
None (Control)	2.6 ± 0.8
<b>Acids</b>	
octanoic acid*	46 ± 8.1
decanoic acid*	89 ± 11.0
oleic acid *	17 ± 2.6
lauric acid*	50 ± 7.5
azelaic acid	1.2 ± 0.1
salicylic acid	5.8 ± 0.4
<i>tert</i> -butyl acetic acid	5 ± 2.3
<b>Ketones</b>	
menthone*	21 ± 2.4
acetophenone	1.4 ± 0.1
4-octanone*	17 ± 2.4
pulegone*	39 ± 7.9
cycloundecanone*	53 ± 5.7
3-methyl-2-hexanone	3.8 ± 2.0
2-methyl cyclohexanone	4.2 ± 1.4
2-heptanone	5.0 ± 0.6
<b>Alcohols</b>	
<i>cis</i> -4-hexen-1-ol*	14 ± 2.3
nonanol*	41 ± 3.8
decanol*	31 ± 6.7
<b>Aldehydes</b>	
hexanal	2.1 ± 0.4
octanal*	28 ± 7.6
salicaldehyde	4.8 ± 0.1
<b>Amines</b>	
N,N-dimethylisopropylamine*	60 ± 8.0
octylamine*	76 ± 8.1
<b>Pyridines/ Pyrrolidones/Pyrrolidinones</b>	
2,4,6-collidine*	10 ± 1.0
1-dodecyl-2-pyrrolidinone*	29 ± 1.5
1-methyl-2-pyrrolidone	7 ± 2.3
2-methyl-3-oxazolidinone	6 ± 1.7
<b>Alkanes/Alkenes/Alkynes</b>	
nonane	4.2 ± 0.3
cyclopentane	3.9 ± 0.1
1-pentene	7 ± 2.6

CPE	RF = $R_0/R_6$
1-pentyne	3.5 ± 0.3
2-methylbutane	2.1 ± 0.2
<b>Halogenoalkanes/alkenes</b>	
1-bromopropane	1.7 ± 0.4
1,2-dichloropropane	3.3 ± 0.8
2,3-dichloro-1-propene*	12 ± 2.4
<b>Other</b>	
cetyltrimethyl ammonium bromide*	19.4 ± 0.1
2-chlorotoluene*	53 ± 7.2
toluene*	16 ± 3.1
dimethyldisulfide*	53 ± 9.0
2-sec-butylphenol *	86 ± 21.7
methyl caproate	6.7 ± 0.7
ethyl 2-methylpentanoate	3.0 ± 0.8
ethylbutyrate	2 ± 1.0

**Table 3**

Cumulative insulin permeated per cm<sup>2</sup>, permeability coefficient (K<sub>p</sub>) values and lag times (L<sub>t</sub>) of insulin in the presence of the CPEs. Values are means and standard deviations of at least three repetitions.

CPE	Insulin		
	Cumulative insulin permeated (IU/cm <sup>2</sup> )	Permeability K <sub>p</sub> (10 <sup>-3</sup> cm/hr)	Lag time L <sub>t</sub> (hr)
none (control)	1.2 ± 0.2	0.7 ± 0.1	6.3 ± 0.9
<b>Acids</b>			
octanoic acid	9 ± 1.6	4.9 ± 0.8	12 ± 2.2
decanoic acid	9 ± 2.7	5 ± 1.4	12 ± 1.8
oleic acid	7 ± 1.3	3.8 ± 0.6	10 ± 1.3
lauric acid	12 ± 4.2	6 ± 2.2	5 ± 2.2
<b>Ketones</b>			
menthone	5 ± 1.2	2.4 ± 0.7	9 ± 2.6
4-octanone	8 ± 1.9	4 ± 1.0	8 ± 3.0
pulegone	3.3 ± 0.5	1.7 ± 0.3	10 ± 2.1
cycloundecanone	10 ± 1.0	5.0 ± 0.4	12 ± 2.4
<b>Alcohols</b>			
<i>cis</i> -4-hexen-1-ol	3.9 ± 0.6	2.4 ± 0.5	12 ± 2.1
nonanol	7 ± 1.1	3.7 ± 0.5	9 ± 1.2
decanol	8.8 ± 0.5	4.6 ± 0.3	7 ± 1.9
<b>Aldehydes</b>			
octanal	10 ± 1.1	5.0 ± 0.6	8 ± 3.0
<b>Amines</b>			
N,N-dimethylisopropyl amine	5 ± 1.8	2.8 ± 0.9	10 ± 1.8
octylamine	7 ± 2.6	4 ± 1.3	10 ± 3.9
<b>Pyridines/ Pyrrolidones/Pyrrolidinones</b>			
2,4,6-collidine	2.5 ± 0.2	1.3 ± 0.1	10 ± 1.3
1-dodecyl-2-pyrrolidinone	2.2 ± 0.2	1.1 ± 0.1	9 ± 1.2
<b>Halogenoalkanes/alkenes</b>			
2,3-dichloro-1-propene	18 ± 1.1	10 ± 1.3	10 ± 0.5
<b>Other</b>			
cetyltrimethyl ammonium bromide	4.7 ± 0.6	2.4 ± 0.3	11 ± 3.3
2-chlorotoluene	14 ± 4.2	8 ± 2.1	9 ± 2.6
toluene	22 ± 5.3	12 ± 5.0	3 ± 1.6
dimethyldisulfide	11 ± 1.2	5.8 ± 0.6	7 ± 1.1
2-sec-butylphenol	11 ± 1.6	5.6 ± 0.8	10 ± 3.2

**Table 4**

Histological evaluation of potential CPEs at 5% w/v concentration

<b>CPE</b>	<b>Grade</b>	<b>CPE</b>	<b>Grade</b>
menthone	D	octanal	A
decanol	B	cycloundecanone	B
oleic acid	A	<i>cis</i> -4-hexen-1-ol	A
4-octanone	B	2,4,6-collidine	A